Progress In Electromagnetics Research B, Vol. 24, 155–172, 2010

SENSITIVITY OF CHIROWAVEGUIDES TO CIRCULAR BIREFRINGENCE BY FIRST ORDER PERTURBATION THEORY

S. Guy, A. Bensalah-Ledoux, and A. Stoita

Laboratoire de Physico-Chimie des Matériaux Luminescents
UMR 5620 CNRS
10 rue Ada Byron, 69622 Villeurbanne cedex, France

Abstract—Planar waveguides with an isotropic chiral core, called chirowaveguides, support the propagation of elliptically polarized modes, making them natural candidates for chiral sensing. We investigate the potential of chirowaveguides as optical sensors responding to changes in the circular birefringence of a medium covering the waveguide. Using first order approximations, we derive expressions for the sensitivities to refractive index and to changes in circular birefringence. The chiral sensitivity is proportional to the achiral sensitivity and to the eccentricity of the mode under consideration. Possible combinations of materials and design conditions for chirowaveguide sensors are discussed with reference to these results. The motivation for this study, besides its theoretical and academic importance, comes from potential applications for enantiomeric integrated optical devices.

1. INTRODUCTION

Handedness or chirality is a symmetry property: an object is chiral if it cannot be superimposed on its mirror image [1]. The two mirror images are called enantiomers. Chirality at the molecular scale plays a fundamental role in living systems for which many mechanisms are based on the selective interaction between chiral active species and chiral receptors. The biological and physiological effects of such enantio-specific interactions can be dramatically affected by the handedness of the enantiomer. Thus, chiral recognition/detection is of prime importance in key areas such as chemical synthesis, catalysis, pharmaceutics and biomedical work.

Received 28 June 2010, Accepted 4 August 2010, Scheduled 12 August 2010
Corresponding author: S. Guy (stephan.guy@univ-lyon1.fr).

Optical chiral recognition takes advantage of one of the aspects characterizing chiral media: the phenomenon of *optical activity*. Polarimeters and circular dichroism spectrometers measure the rotatory power α and the differential absorption between left- and right-circularly polarized light, respectively. These techniques are of proven efficiency but are limited to off-line analysis.

The concept of a solid miniaturized chiral sensor opens exciting perspectives in process monitoring. Recently, the differential detection of isomers was demonstrated using an organic thin-film transistor gas sensor [2]. The chiral discrimination arises from in-diffusion and the subsequent capture of target molecules in the outermost chiral layer. This capture-based sensing depends on finding a good receptor-analyze association.

Research for a more versatile compact chiral sensor involves the direct detection of a physical parameter related only to chirality. The most universal parameter is circular birefringence, $c_b = n_L - n_R$, where n_L and n_R are the refractive indices for left- and right-circularly polarized waves illuminating the material. It vanishes for non-chiral media and changes sign with the enantiomer.

In order to directly measure this parameter, it is necessary to use an optical device capable of supporting the propagation of circularly polarized waves. Chirowaveguides, or planar waveguides with an isotropic chiral core [3], are natural candidates for such a task because they allow the propagation of circularly polarized waves [4]. This new class of waveguides was proposed for the first time in 1989 [3] and, since then, a lot of theoretical work has been done in order to determine their modal properties [4–7]. Recently, thin films based on binaphthyl molecules featuring high isotropic optical rotation have been synthesized, opening the way to the practical realization of chirowaveguides [8–10].

In this paper, we investigate theoretically the potential of chirowaveguides to act as circular birefringence optical sensors. The idea is to combine the compactness and flexibility of evanescent planar wave sensors [11] with the unique ability of chirowaveguides to support the propagation of circularly polarized waves. Basic optical waveguide sensor devices are fabricated from a thin film of high refractive index, the core, coated on a substrate of lower index. The chemically sensitive material is applied as a cladding layer on "top" of the waveguide and is probed by the evanescent field of the mode [12]. In the main, optical sensors probe three different physical parameters (fluorescence, absorption and refractive index). Here, we focus on the measurement of refractive index: a variation of the refractive index in the region probed by the evanescent field induces a variation of the effective refractive

index of the guided wave. In the case of chiro-sensing, two parameters may impact on the modal properties: the *achiral* refractive index — correlated to permittivity — and the *chiral* circular birefringence.

Whatever optical device is used as refractive waveguide sensor (interferometer, resonator or mode coupler), the first design task is to find the waveguide structure which maximizes the sensitivity to the quantity that needs to be measured [13]. Various papers [11, 13] have been published on how to accomplish this task for achiral waveguides. The goal of this work is to decide whether or not chirowaveguides may be used as circular birefringence sensors. The first issue is to find a waveguide structure with good sensitivity to circular birefringence. Theoretically, the first step is then to derive an expression for the sensitivity to this chiral property. We denote this sensitivity by S_{chir}. The second issue comes from the fact that the circular birefringence is many orders of magnitude smaller than the refractive index. Thus, the achiral sensitivity S_{achi} to refractive index also needs to be calculated and compared to S_{chir}. If $S_{achi} \neq 0$, refractive index sensing will overwhelm chiral sensing and a special set-up that cancels S_{achi} must be conceived.

The paper is organized as follows: the first part is dedicated to the formulation of the electromagnetic problem and introduces the notation. In the second part, expressions for the sensitivities are derived using perturbation theory. In the following section, we write the sensitivities as a function of one transverse electric field component. In Section 4, we provide some leads on how to optimize S_{chir}. Finally, we show that a difference interferometer achieves the cancellation of achiral sensing.

2. FORMULATION OF THE PROBLEM

We consider an isotropic nonmagnetic chiral medium. Its electromagnetic constants are the relative permittivity ϵ and the chiral parameter γ. By taking the time variation of the fields in the form $\exp(i\omega t)$, the fields $\mathbf{E}$ and $\mathbf{H}$ satisfy the Maxwell equations:

$$\nabla \times \mathbf{E} = -i\omega\mathbf{B} \qquad \nabla \times \mathbf{H} = i\omega\mathbf{D} \tag{1}$$

We adopt constitutive equations including chirality in the Drude-Born-Federov form [14]:

$$\mathbf{D} = \epsilon\left(\mathbf{E} + \gamma\nabla \times \mathbf{E}\right) \tag{2}$$

$$\mathbf{B} = \mu_0\left(\mathbf{H} + \gamma\nabla \times \mathbf{H}\right) \tag{3}$$

Plane waves propagating in such media are right-handed circularly or

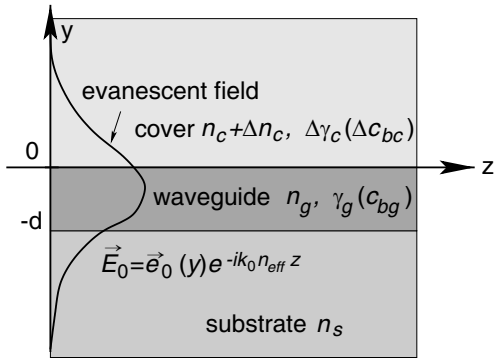

Figure 1. Schematic representation of a slab chirowaveguide sensor.

left-handed circularly polarized with refractive index $n_{R/L}$ [14]:

$$n_{R/L} = \frac{n}{1 \pm k_0 n\gamma} \tag{4}$$

$$n^2 = \epsilon/\epsilon_0 \quad k_0^2/\omega^2 = \epsilon_0\mu_0 \tag{5}$$

The chiral parameter being very small, the circular birefringence may be approximated as

$$c_b = 2n^2 k_0 \gamma \tag{6}$$

The circular birefringence is related to rotary power by $\alpha = k_0 c_b/2$ [15].

The structure of the waveguide under consideration is shown in Fig. 1. The core, of thickness d, and the cover are chiral with refractive indices n_g and n_c, respectively. Their chiral parameters are γ_g and $\Delta\gamma_c$, respectively, with corresponding circular birefringences c_{bg} and Δc_{bc}. The refractive index of the achiral substrate is n_s. The planar waveguide is invariant over the x and z axes, and the axis of the waveguide is taken as the z axis.

We are looking for the solution of the problem represented by the structure with parameters $(n_s,\ n_g,\ c_{bg},\ n_c + \Delta n_c,\ \Delta c_{bc})$ where Δn_c is a small variation in the cover refractive index. We assume that the cover chiral parameter is much smaller than the core chiral parameter. Indeed, the design of a chirowaveguide requires materials with a much higher rotary power than a conventional diluted chiral medium [4]. Under these assumptions ($\Delta n_c \ll n_c$ and $\Delta c_{bc} \ll c_{bg}$), we treat the problem using perturbation theory. The unperturbed structure is a chirowaveguide with parameters $(n_s,\ n_g,\ c_{bg},\ n_c,\ \Delta c_{bg} = 0)$. The general solution for modes in such an asymmetric chirowaveguide was given by Herman in [4]. The modes are no longer split between Transverse Electric (TE) and Transverse Magnetic (TM) modes, but

between LHE (Left Hand Elliptical) and RHE (Rigth Hand Elliptical) modes. The transverse polarization of a given mode is linear at the cutoff and elliptical for greater thickness. The eccentricity of the polarization ellipse of the transverse electric field increases with core thickness up to circular polarization for large thicknesses.

The electromagnetic fields satisfy Equations (1)–(3) where ϵ and γ are functions of the y coordinate. The $\gamma(y)$ and $\epsilon(y)$ functions describing the chirowaveguide sensor are plotted in Fig. 2(a). They can be written as:

$$\epsilon(y) = \epsilon_u(y) + \Delta\epsilon(y) \tag{7}$$

$$\gamma(y) = \gamma_u(y) + \Delta\gamma(y) \tag{8}$$

where $\epsilon_u(y)$, $\gamma_u(y)$ are the electromagnetic functions describing the unperturbed chirowaveguide structure (parameters given in Fig. 2(b)) and $\Delta\gamma(y)$, $\Delta\epsilon(y)$ are the electromagnetic perturbations defined in Fig. 2(c).

We use the independent variables ϵ and γ and their pertrubation in the first order perturbation theory (Appendix A). Nevertheless, to get a better physical meaning, the final result is given in term of the

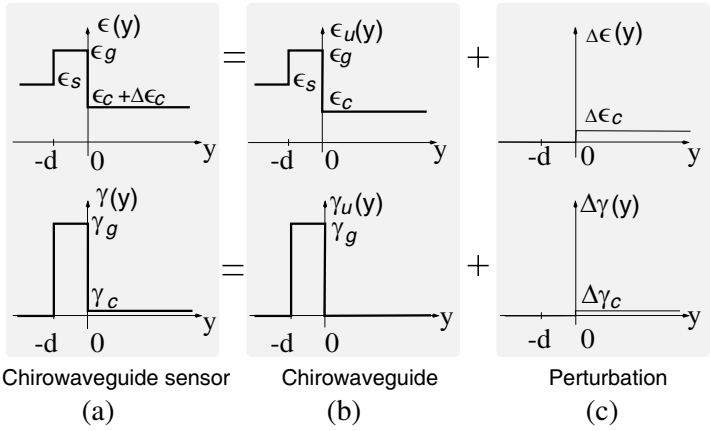

Figure 2. Variation of electromagnetic functions $\epsilon(y)$ and $\gamma(y)$ with y for (a) chirowaveguide sensor, (b) unperturbed chirowaveguide and (c) perturbation.

two independent perturbed cover parameters:

$$\Delta n_c = \left(\frac{\partial n}{\partial \epsilon}\right) \Delta \epsilon_c \tag{9}$$

$$\Delta c_{bc} = \left(\frac{\partial c_b}{\partial \gamma}\right) \Delta \gamma \tag{10}$$

Using (5) and (6), those perturbed parameters can be written:

$$2n_c \epsilon_0 \Delta n_c = \Delta \epsilon_c \tag{11}$$

$$\Delta c_{bc} = 2n_c^2 k_0 \Delta \gamma_c \tag{12}$$

Let

$$\mathbf{E}_0 = \mathbf{e}_0(y) e^{-ik_0 n_{eff} z} \tag{13}$$

be the solution of one mode of the unperturbed chirowaveguide, where n_{eff} is the effective index of the mode. We assume that the application of perturbations $\Delta\epsilon(y)$, $\Delta\gamma(y)$ will only cause small changes to the mode function $\mathbf{e}_0(y)$ and effective index n_{eff}. Let

$$\mathbf{E}_p = \mathbf{e}_p(y) e^{-ik_0 n_{eff,p} z} \tag{14}$$

be the corresponding perturbed mode, where:

$$\mathbf{e}_p(y) = \mathbf{e}_0(y) + \Delta \mathbf{e}_0(y) \tag{15}$$

$$n_{eff,p} = n_{eff} + \Delta n_{eff} \tag{16}$$

$\Delta \mathbf{e}_0(y)$ and Δn_{eff} are the first order changes in the mode function and effective refractive index, respectively. Mathematically speaking, assuming that the changes in the cover parameters are small, the resulting change in the effective refractive index can be described to first order by:

$$\Delta n_{eff} = S_{achi} \Delta n_c + S_{chir} \Delta c_{bc} \tag{17}$$

S_{achi} is the sensor sensitivity to a change in cover refractive index. S_{chir} is the sensor sensitivity to a change in cover circular birefringence. S_{chir} probes the chiral electromagnetic parameter of the cover and S_{achi} probes the achiral parameter.

3. SENSITIVITIES VERSUS ONE TRANSVERSE FIELD COMPONENT

3.1. Results of Perturbation Theory

The use of the Lorentz reciprocity theorem is needed to obtain the relationship between the unperturbed and perturbed fields. In the conventional way [15, 16], we must develop the expression

$$\nabla \cdot (\mathbf{E}_0^* \times \mathbf{H}_p + \mathbf{E}_p \times \mathbf{H}_0^*) \tag{18}$$

where * denotes the complex conjugate and integrate it over the waveguide cross-section. The details of the calculations are given in the appendix and follow the procedure given in [16]. The identification of (A11) with (17) leads to expressions for the sensitivities:

$$S_{chir} = \frac{i}{8P_u} \int_0^{+\infty} (\mathbf{E}_0 \cdot \mathbf{H}_0^* - \mathbf{H}_0 \cdot \mathbf{E}_0^*)\, dy \tag{19}$$

$$S_{achi} = \frac{1}{2P_u} \int_0^{+\infty} \frac{n_c}{\eta_0} \mathbf{E}_0 \cdot \mathbf{E}_0^* dy \tag{20}$$

where P_u is the power propagating in the unperturbed waveguide defined by (A12).

3.2. Sensistivity Versus Mode Eccentricity

In achiral films, as is well known, the modes are separated into TE and TM linear polarization types. In a chirowaveguide, the modes are also split into two families of modes. Both have transverse elliptical polarizations outside the core. The two families of modes are differentiated by their handedness (left or right) and by the direction of the major axis of the transverse polarization ellipse ($\hat{\mathbf{x}}$ or $\hat{\mathbf{y}}$) [4]. The class of mode with major axis along the x direction tends to be the TE modes for small γ_g chirality parameter. For positive values of γ_g, they are LHE polarized. Modes with major axis lying along the y direction tend to be TM modes in the weak chirality limit and are RHE polarized for $\gamma_g > 0$.

The eccentricity of the polarization ellipse in the cover is defined by:

$$\left.\frac{E_y}{E_x}\right|_{y\geq 0} = ie_c \tag{21}$$

For $|e_c| \leq 1$, the major axis of the polarization ellipse lies along the x direction, for larger values it lies along the y direction. The sign of e_c gives the handedness. The limit values 0, ± 1 and $\pm\infty$ correspond to TE, circular and TM polarizations, respectively. Using the results of Ref. [4] (Eqs. (3), (8) and (11)), the field coordinates in the top cladding for the unperturbed mode can be written as a function of the E_x component only:

$$\mathbf{E}_0 = E_x(y) \begin{pmatrix} 1 \\ ie_c \\ -ve_c/n_{eff} \end{pmatrix} \tag{22}$$

$$\mathbf{H}_0 = E_x(y)\frac{1}{\eta_0 n_{eff}}\begin{pmatrix} -in_c^2 e_c \\ n_{eff}^2 \\ ivn_{eff} \end{pmatrix} \tag{23}$$

where:

$$v^2 = n_{eff}^2 - n_c^2, \qquad E_x(y) = E_x(0)\exp(-k_0 vy) \tag{24}$$

Substituting (22)–(23) in S_{chir} (19) and S_{achi} (20) leads to:

$$S_{chir} = -S_0 \cdot \frac{n_{eff}}{n_c} \cdot e_c \tag{25}$$

$$S_{achi} = S_0 \cdot \left[1 + e_c^2\left(2 - n_c^2/n_{eff}^2\right)\right] \tag{26}$$

where:

$$S_0 = \frac{\int_0^{+\infty} n_c E_x E_x^* dy}{2\eta_0 P_u} \tag{27}$$

is the sensitivity of a "standard" achiral waveguide [12, 15]. These expressions hold whatever the polarization, nevertheless they lead to an indeterminate situation in the TM limit for which $E_x \to 0$ and $e_c \to \infty$. Thus, for an elliptically polarized mode with major axis lying along the y axis, it is advantageous to change to a new eccentricity:

$$\bar{e}_c = 1/e_c \tag{28}$$

For $|\bar{e}_c| < 1$, the transverse electric field is elliptically polarized with major axis lying along the y axis and $\bar{e}_c = 0$ corresponds to the TM limit. In the same manner as before, we find:

$$S_{chir} = -\bar{S}_0 \cdot \frac{n_{eff}}{n_c} \cdot \bar{e}_c \tag{29}$$

$$S_{achi} = \bar{S}_0 \cdot [2 - n_c^2/n_{eff}^2 + \bar{e}_c^2] \tag{30}$$

where :

$$\bar{S}_0 = \frac{\int_0^{+\infty} n_c E_y E_y^* dy}{2\eta_0 P_u} \tag{31}$$

4. DISCUSSION

The sensitivities to an uniform chiral and achiral perturbation in the cover refractive index are given in general form by (19) and (20), respectively. To gain a deeper understanding of the phenomenon, we have calculated the expressions of S_{chir} and S_{achi} as a function of one transverse electric field component ((25)–(31)).

In the following paragraphs, we will first analyze these expressions in order to get the general features of the chirowaveguide sensitivities.

Then, we will discuss the different possibilities leading to significant values for chiral sensitivity.

For this last purpose, we have generated a computer program to calculate sensitivity curves for different model systems. The mode equation and field patterns are taken from the paper of Herman [4]. The numerical simulations use a light-source wavelength of 500 nm and a positive chiral parameter for the core. The chirality of the core was studied for rotary power values between 0 and 50°/mm. The LHE modes present polarization ellipses with major axis lying along the x direction. The RHE modes' polarization ellipses have their longer axes oriented in the y direction. The numerical results are presented only for the fundamental LHE_0 and RHE_0 modes, the higher modes behave in a similar way with smaller values for the sensitivities.

4.1. General Features

4.1.1. Achiral Sensitivity

Equation (20) shows that the achiral sensitivity is related to the integral of the squared evanescent field in the cover material. This result is identical to that obtained for achiral waveguides [13, 15]. S_{achi} thus has no direct dependence on the chirality of the chirowaveguide. Fundamentally, this comes from the fact that the perturbation $\Delta\epsilon(y)$ does not couple with the chirality parameters in the expression for the field curls in (A3)–(A4).

The expression (20) only depends on the electric field modal profiles. Thus S_{achi} may depend on the chirality only via a change in the field patterns between chirowaveguide and achiral waveguide. We check this point by plotting the field patterns and S_{achi} for chirowaveguides with rotary power varying from 0 to 80°/mm for various refractive indices and thicknesses. Our simulations did not reveal any detectable variation with the chirality of the core. Thus, we can safely conclude that chirowaveguides behave like achiral waveguides in terms of achiral sensing.

4.1.2. Chiral Sensitivity

The general expression for chiral sensitivity (19) shows that it depends on the field polarisation structure via the scalar product $\mathbf{E}_0 \cdot \mathbf{H}_0^*$. For standard TE/TM modes this product is zero showing that achiral waveguides cannot sense chirality in the cover. In a chirowaveguide, $\mathbf{E}$ and $\mathbf{H}$ are no longer perpendicular, thus chiral sensing is possible.

The expressions for S_{chir} as a function of one transverse electric field component (E_x, (25) and E_y, (29)) reveal that S_{chir} can be

factorized into two terms: one term proportional to achiral sensitivity (S_0 or $\bar{S}_0$) and another term proportional to the eccentricity (e_c or $\bar{e}_c$) of the transverse polarization ellipse. In this discussion, we can neglect the term n_{eff}/n_c which is limited between n_s/n_c and n_g/n_c and does not vary significantly compared to the eccentricity.

The first term depends only on the mode profiles and not on the chirality as stated before. It represents the fraction of the power propagating in the perturbed cover. The second term, the eccentricity, is directly related to the chiral nature of chirowaveguides. Its sign changes with the handedness of the propagating mode and vanishes for achiral waveguides.

4.2. Chiral Sensitivity Optimization

The optimization of chiral sensitivity requires the *simultaneous* optimization of two different terms: the "standard" achiral sensitivity (via the terms S_0, $\bar{S}_0$) and the eccentricity (e_c, $\bar{e}_c$). The first term is generally maximized by using a combination of materials leading to high contrast in refractive index ($\Delta n \sim 0.3$) and by working with thin guiding layers (thicknesses of a few hundreds of nm) [11]. The eccentricity, on the other hand, takes significant values in chirowaveguides with high rotary power, small index contrast and thick cores [4].

Figures 3 and 4 illustrate the difficulties in finding a good trade-off between the two constraints. In both figures, the calculated S_{achi}, S_{chir} and eccentricity curves versus core thickness are plotted in the (a), (b) and (c) sub-figures respectively. We choose, as chiral core parameters, a refractive index of 1.75 and a rotary power of 20°/mm. These values are taken from pure chiral organic thin films deposited by pulsed laser ablation [10]. The cover is an aqueous medium ($n_c = 1.33$). The difference between the two figures comes from the substrate refractive index: 1.48 and 1.74 for Figs. 3 and 4 respectively.

The large difference between refractive indices in the first case allows good achiral sensitivity ($S_{achi} \sim 0.15$) for thicknesses less than 200 nm. But, as the eccentricity is lower than 10^{-3} in this range of thicknesses, this results in small S_{chir}. For greater thicknesses, the eccentricity increases, but not enough to compensate for the fall in S_{achi}. Finally, whatever the thickness, S_{chir} remains small, less than 10^{-4}.

In the second example, by reducing the contrast in refractive index between core and substrate, the chiral feature of the chirowaveguide is emphasized (the eccentricity is twice as high for the same chirality in the core Figs. 3(c) and 4(c). But, at the same time, S_{achi} is

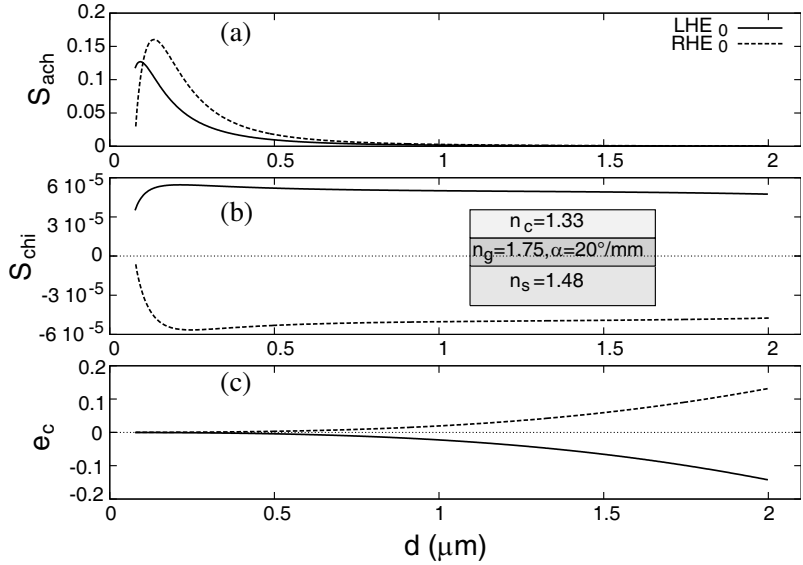

Figure 3. Calculated sensitivities of evanescent-wave chirowaveguide sensor, depending on waveguide film thickness, for chiral core ($\alpha = 20°$/mm, $n_g = 1.75$) on achiral substrate ($n_s = 1.48$). Sensitivities to (a) changes in refractive index ($n_c = 1.33$) of aqueous cover medium, and (b) changes of circular birefringence (n_L-n_R) of cover. (c) Calculated tranverse ellipticities of the modes (ratio of small axis over large axis).

dramatically decreased by about 2 orders of magnitude. Thus, again, the chiral sensitivity is very weak ($< 10^{-4}$).

One way to optimize a chirowaveguide sensor is to use nearly symmetrical waveguides with low refractive index contrast. Indeed, (1) high *achiral* sensitivity may be achieved with nearly symmetrical waveguides due to the equal extent of the modal field outside the core [17] and (2) the smaller the index contrast, the higher the eccentricity [4]. The second condition will limit the use of chirowaveguides to special cover/core/substrate material combinations with small index differences. As it is difficult to realize solid materials with $n_g < 1.4$, we use, in the following, a cover refractive index $n_c = 1.5$ corresponding to an organic solvent.

Maximum achievable chiral sensitivities versus refractive index contrasts are shown in Fig. 5 in the case of a cover refractive index $n_c = 1.5$ and core rotary power of 20°/mm. These curves show clearly that, the smaller the refractive index contrast (for both $n_g - n_s$ and

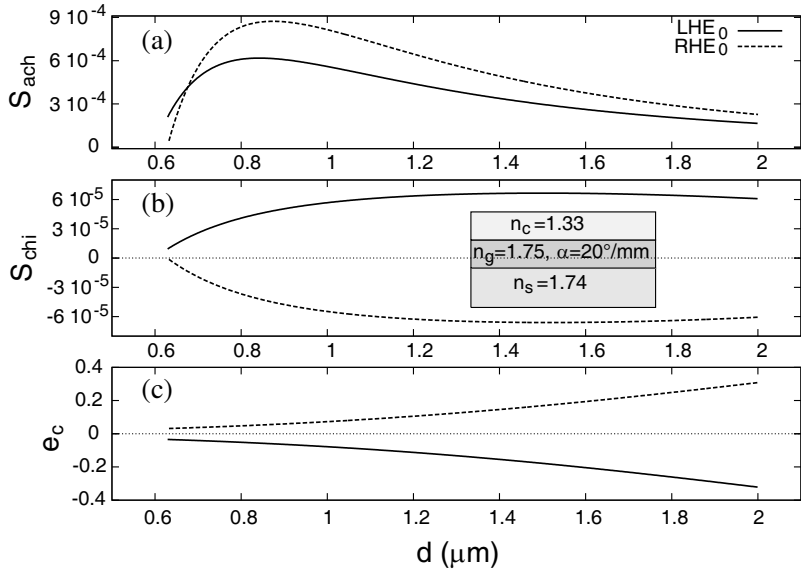

Figure 4. Calculated sensitivities of evanescent-wave chirowaveguide sensor, depending on waveguide film thickness, for chiral core ($\alpha = 20°/\text{mm}$, $n_g = 1.75$) on achiral substrate ($n_s = 1.74$). Sensitivities to (a) changes in refractive index ($n_c = 1.33$) of aqueous cover medium, and (b) changes of circular birefringence (n_L-n_R) of cover. (c) Calculated transverse ellipticities of the modes (ratio of small axis over large axis).

$n_g - n_c$), the higher S_{chir} is. Theoretical sensitivities higher than 0.02 (circle and square curves) are achievable but they require a very small difference in index ($n_s - n_c \sim 10^{-3}$), necessitating accurate control of materials.

A higher rotary power will obviously simplify the refractive index constraints, as shown in Fig. 6, where the maximum achievable sensitivities are plotted versus α for a given chirowaveguide (parameters $n_g = 1.52$, $n_s = 1.51$ and $n_c = 1.5$). Indeed, S_{chir} increases with α allowing good sensitivities to be achieved with higher index contrast.

In order to further increase the sensitivities, a reverse-symmetry waveguide ($n_c > n_s$) can be used [13, 17, 18]. Calculated sensitivities of the same chirowaveguide used in standard (top) and reverse-symmetry (bottom) modes, are plotted in the Fig. 7. As expected from previous works [18], S_{achi} is significantly enhanced by about one order of magnitude in the reverse-symmetry mode. Because the eccentricity

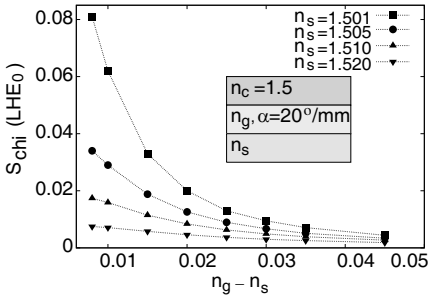

Figure 5. Calculated maximum achievable chiral sensitivity S_{chir} versus index contrast $n_g - n_s$ of the fundamental LHE mode. The various curves correspond to different values of the substrate refractive index. The core rotary power is 20°/mm and the refractive index of the cover is $n_c = 1.5$.

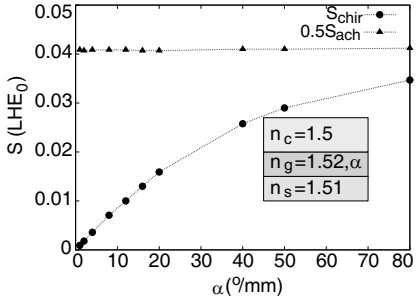

Figure 6. Maximum achievable sensitivities versus α. The waveguide is made up of a chiral core (α, $n_g = 1.52$), an achiral substrate ($n_s = 1.51$) and a chiral cover ($n_c = 1.5$).

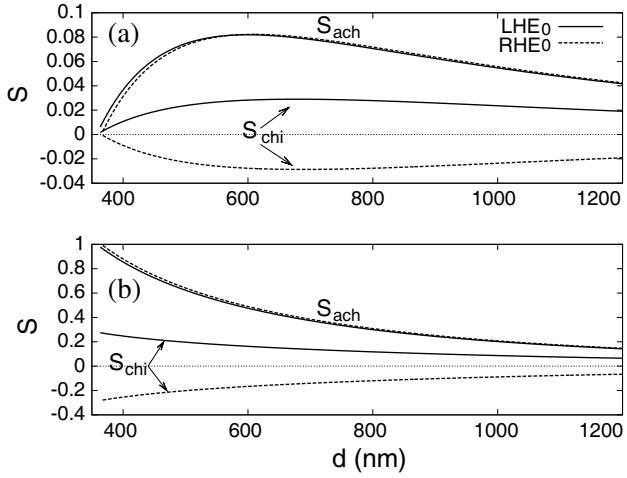

Figure 7. Calculated sensitivities of evanescent-wave chirowaveguide sensor versus waveguide film thickness for chiral core ($\alpha = 50°$/mm, $n_g = 1.52$). At the top, a normal-symmetry chirowaveguide is used for the calculations ($n_s = 1.51$, $n_c = 1.5$). At the bottom, reverse symmetry is used ($n_s = 1.5$, $n_c = 1.51$).

remains identical in the two modes, S_{chir} is enhanced by the same factor, reaching values as high as 0.2 as shown in Fig. 7.

4.3. Chirowaveguide as Difference Interferometer

Nevertheless, an issue remains: the order of magnitude of the circular birefringence c_b is very small compared to the standard achiral refractive index. For a typical chiral organic compound, such as glucose ($[\alpha]_D = 52.9^\circ\ \mathrm{g}^{-1} \cdot \mathrm{ml} \cdot \mathrm{dm}^{-1}$), the circular birefringence is of the order of 10^{-7} at visible wavelengths for a concentration around $0.1\,\mathrm{g} \cdot \mathrm{ml}^{-1}$. Any fluctuation of the cover refractive index will easily overwhelm the circular birefringence. Thus, the only way to actually detect changes in chirality requires the cancellation of achiral sensing.

For this purpose, a solution is to use chirowaveguides as difference interferometers, also called polarimeters [19]. For this detection set-up, the measurement is the phase difference between two modes propagating in the waveguide. Thus, by working with the LHE_0 and RHE_0 pair of modes, the measurement is directly proportional to the effective refractive index difference $\widetilde{n_{eff}} \equiv n_{eff}^{LHE_0} - n_{eff}^{RHE_0}$. Using (17), the index difference is related to the various sensitivities by:

$$\Delta\widetilde{n_{eff}} = (S_{achi}^{LHE_0} - S_{achi}^{RHE_0})\Delta n_c + (S_{chir}^{LHE_0} - S_{chir}^{RHE_0})\Delta c_{bc} \qquad (32)$$

where the RHE_0 and LHE_0 superscripts refer to the RHE_0 and $\mathrm{L}HE_0$ modes, respectively. As the LHE_0 and RHE_0 achiral sensitivities include cross-terms, it is easy to cancel out the achiral part in (32) by designing the core thickness in such a way that $S_{achi}^{LHE_0} = S_{achi}^{RHE_0}$ (for example 560 nm in the top of Fig. 7). Moreover, while the achiral sensitivity vanishes, the chiral sensitivity is twice as high as can be seen in Fig. 7.

5. CONCLUSION

The potential for using chirowaveguides as refractometric optical sensors was investigated. For the first time, an expression for the chirowaveguide sensitivity as a function of both the refractive index and circular birefringence of the cover was obtained using perturbation theory. The following features were revealed:

- chirowaveguides act as standard achiral waveguides for achiral sensing;
- the chiral sensitivity S_{chir} is written as the product of achiral sensing and mode eccentricity;

- optimization of chiral sensitivity requires the use of a waveguide with small contrast in refractive index.

The requirement for small refractive index contrast devices limits the general use of chirowaveguides as refractive sensors. Indeed, the indices of the chiral core and cover medium (analyze) need to be very close to equal, making gas or aqueous sensing irrelevant. Some applications can be found in organic environments with higher refractive index. Numerical simulations show that good sensitivities can be obtained when probing a medium of index around 1.5. Sensitivity values of 0.02 and 0.2 can be achieved using normal or reverse-symmetry configurations, respectively.

Finally, in practical applications, fluctuations of the refractive index of the medium may overwhelm chiral sensing except if achiral sensing is cancelled in identical fashion. We have suggested a difference interferometer design to totally suppress the achiral component in refractometric sensing.

ACKNOWLEDGMENT

This work was supported by the Agence Nationnale de la Recherche, grant number ANR-08-BLAN-0149-01.

APPENDIX A. PERTURBATION THEORY

Substituting the constitutive Equations (2) and (3) in the Maxwell Equation (1) and keeping only the first order term in γ_u, we obtain for the unperturbed fields (remember here ϵ_u and γ_u are functions of y):

$$\nabla \times \mathbf{E}_0 = -i\omega\mu_0\mathbf{H}_0 + \mu_0\epsilon_u\omega^2\gamma_u\mathbf{E}_0 \quad \text{(A1)}$$

$$\nabla \times \mathbf{H}_0 = \mu_0\epsilon_u\omega^2\gamma_u\mathbf{H}_0 + i\omega\epsilon_u\mathbf{E}_0 \quad \text{(A2)}$$

For the perturbed fields, by neglecting the second order terms and noting that $\Delta\epsilon(y)\gamma_u(y) = 0$, we obtain in the same way:

$$\nabla \times \mathbf{E}_p = -i\omega\mu_0\mathbf{H}_p + \mu_0\epsilon_u\omega^2(\gamma_u + \Delta\gamma)\mathbf{E}_p \quad \text{(A3)}$$

$$\nabla \times \mathbf{H}_p = \mu_0\epsilon_u\omega^2(\gamma_u + \Delta\gamma)\mathbf{H}_p + i\omega(\epsilon_u + \Delta\epsilon)\mathbf{E}_p \quad \text{(A4)}$$

By substituting the curl term from (A1)–(A4) and assuming that the media are lossless, we can write:

$$\nabla \cdot (\mathbf{E}_0^* \times \mathbf{H}_p) = \mathbf{H}_p \cdot \nabla \times \mathbf{E}_0^* - \mathbf{E}_0^* \cdot \nabla \times \mathbf{H}_p$$
$$= i\omega\mu_0\mathbf{H}_p \cdot \mathbf{H}_0^* - \mu_0\epsilon_u\omega^2\Delta\gamma\mathbf{E}_0^* \cdot \mathbf{H}_p - i\omega\left(\epsilon_u + \Delta\epsilon\right)\mathbf{E}_p \cdot \mathbf{E}_0^* \quad \text{(A5)}$$

and :

$$\begin{aligned}\nabla \cdot (\mathbf{E}_p \times \mathbf{H}_0^*) &= \mathbf{H}_0^* \cdot \nabla \times \mathbf{E}_p - \mathbf{E}_p \cdot \nabla \times \mathbf{H}_0^* \\ &= -i\omega\mu_0 \mathbf{H}_0^* \cdot \mathbf{H}_p + \mu_0 \epsilon_u \omega^2 \Delta\gamma \mathbf{E}_p \cdot \mathbf{H}_0^* + i\omega\epsilon_u \mathbf{E}_p \cdot \mathbf{E}_0^* \end{aligned} \quad \text{(A6)}$$

Adding these two terms leads to the identity:

$$\begin{aligned}&\nabla \cdot (\mathbf{E}_0^* \times \mathbf{H}_p + \mathbf{E}_p \times \mathbf{H}_0^*) \\ &= \mu_0 \epsilon_u \omega^2 \Delta\gamma \left(\mathbf{E}_p \cdot \mathbf{H}_0^* - \mathbf{E}_0^* \cdot \mathbf{H}_p\right) - i\omega\Delta\epsilon \mathbf{E}_p \cdot \mathbf{E}_0^* \end{aligned} \quad \text{(A7)}$$

As the function $\Delta\gamma(y)$ vanishes for $y < 0$, $\epsilon_u(y)$ can be replaced by ϵ_c in this expression. Then, by using (5), (11) and (12), it can be written as a function of $\Delta c_b(y)$ and $\Delta n(y)$:

$$\begin{aligned}&\nabla \cdot (\mathbf{E}_0^* \times \mathbf{H}_p + \mathbf{E}_p \times \mathbf{H}_0^*) \\ &= \frac{k_0}{2} \left(\mathbf{E}_p \cdot \mathbf{H}_0^* - \mathbf{E}_0^* \cdot \mathbf{H}_p\right) \Delta c_b(y) - \frac{2in(y)k_0}{\eta_0} \mathbf{E}_p \cdot \mathbf{E}_0^* \Delta n(y) \end{aligned} \quad \text{(A8)}$$

where $\eta_0 = \sqrt{\mu_0/\epsilon_0}$.

Taking into account the z, y dependencies of the fields $\mathbf{E}_0$ (13) and $\mathbf{E}_p$ (14) together with (16), the ∇ in (A8) simplifies to:

$$\nabla = \frac{\partial}{\partial y} \hat{\mathbf{y}} - ik_0 \Delta n_{\mathit{eff}} \hat{\mathbf{z}} \quad \text{(A9)}$$

where $\hat{\mathbf{y}}$ and $\hat{\mathbf{z}}$ are the unit vectors in the y and z directions. Since the modes are confined, the integral

$$\int_y \frac{\partial}{\partial y} \hat{\mathbf{y}} \cdot (\mathbf{E}_0^* \times \mathbf{H}_p + \mathbf{E}_p \times \mathbf{H}_0^*)\, dy = 0 \quad \text{(A10)}$$

Thus, by integrating (A8) over the entire y axis with (A9)–(A10), and substituting the unperturbed fields for the perturbed fields, we obtain:

$$\begin{aligned}\Delta n_{\mathit{eff}} &= \frac{i}{8P_u} \int_{-\infty}^{+\infty} \Delta c_b(y) \left(\mathbf{E}_0 \cdot \mathbf{H}_0^* - \mathbf{H}_0 \cdot \mathbf{E}_0^*\right) dy \\ &\quad + \frac{1}{2P_u} \int_{-\infty}^{+\infty} \Delta n(y) \frac{n_c}{\eta_0} \mathbf{E}_0 \cdot \mathbf{E}_0^* dy \end{aligned} \quad \text{(A11)}$$

where the factor in the denominator represents the power propagating in the unperturbed waveguide:

$$4P_u = \int_{-\infty}^{+\infty} \hat{\mathbf{z}} \cdot (\mathbf{E}_0^* \times \mathbf{H}_0 + \mathbf{E}_0 \times \mathbf{H}_0^*)\, dy \quad \text{(A12)}$$

(A11) can be directly identified with (17) by noting that the $\Delta n(y)$ and $\Delta c_b(y)$ functions vanishes for $y < 0$ and are constant above (Fig. 2(c)).

REFERENCES

1. Barron, L. D. *Molecular Light Scattering and Oprical Activity*, Cambridge University Press, Cambridge, 2004.
2. Torsi, L., G. M. Farinola, F. Marinelli, M. C. Tanese, O. H. Omar, L. Valli, F. Babudri, F. Palmisano, P. G. Zambonin, and F. Naso, "A sensitivity-enhanced field-effect chiral sensor," *Nat. Mater.*, Vol. 7, No. 5, 412–417, 2008.
3. Engheta, N. and P. Pelet, "Modes in chirowaveguides," *Opt. Lett.*, Vol. 14, No. 11, 593–595, 1989.
4. Herman, W. N., "Polarization eccentricity of the transverse field for modes in chiral core planar waveguides," *J. Opt. Soc. Am. A*, Vol. 18, No. 11, 2806–2818, 2001.
5. Pelet, P. and N. Engheta, "The theory of chirowaveguides," *IEEE Trans. Antennas Prop*, Vol. 38, No. 1, 90–98, January 1990.
6. Demidov, S. V., K. V. Kushnarev, and V. V. Shevchenko, "Dispersion properties of the modes of chiral planar optical waveguides," *J. Comm. Tech. Electron.*, Vol. 44, 827–832, 1999.
7. Bahar, E., "Mueller matrices for waves reflected and transmitted through chiral materials: Waveguide modal solutions and applications," *J. Opt. Soc. Am. B*, Vol. 24, 1610–1619, 2007.
8. Herman, W. N., "Amorphous thin films of chiral binaphtyls for photonic waveguides," *J. Macromol. Sci., Part A, Pure Appl. Chem.*, Vol. 40, No. 12, 1369–1382, 2003.
9. Guy, L., T. Vautey, and S. Guy, "The use of $LCMS$ as an analytical tool for hydrolysis/polycondensation monitoring of a chiral ormosil precursor," *Sol. Gel. Science Technologie*, Vol. 52, 146–152, 2009.
10. Guy, S., L. Guy, A. Bensalah, A. Pereira, V. Grenard, O. Cosso, and T. Vautey, "Pure chiral organic thin films with high isotropic optical activity synthesized by UV pulsed laser deposition," *J. Mater. Chem.*, Vol. 19, 7093–7097, 2009.
11. Lambeck, P. V., "Integrated optical sensors for the chemical domain," *Meas. Sci. Technol.*, Vol. 17, No. 8, R93–R116, 2006.
12. Lukosz, W., "Principles and sensitivities of integrated optical and surface plasmon sensors for direct affinity sensing and immunosensing," *Biosensors and Bioelectronics*, Vol. 6, No. 3, 215–225, 1991.
13. Tiefenthaler, K. and W. Lukosz, "Sensitivity of grating couplers as integrated-optical chemical sensors," *J. Opt. Soc. Am. B*, Vol. 6, No. 2, 209–220, 1989.

14. Lindell, V. I., A. Shivola, S. A. Tretyakov, and A. J. Viitanen, *Electromagnetic Waves in Chiral and Bi-isotropic Media*, Artech House, 1994.
15. Yariv, A. and P. Yeh, *Optical Waves in Crystals*, Wiley, New York, 1984.
16. Pelet, P. and N. Engheta, "Coupled-mode theory for chirowaveguides," *J. Appl. Phys.*, Vol. 67, No. 6, 2742–2745, 1990.
17. Parriaux, O. and G. J. Veldhuis, "Normalized analysis for the sensitivity optimization of integrated optical evanescent-wave sensors," *J. Lightwave Technol.*, Vol. 16, No. 4, 573–582, 1998.
18. Horvath, R., L. R. Lindvold, and N. B. Larsen, "Reverse-symmetry waveguides: Theory and fabrication," *Appl. Phys. B*, Vol. 74, 383–93, 2002.
19. Lukosz, W., "Integrated optical chemical and direct biochemical sensors," *Sensors and Actuators B*, Vol. 29, 37–50, 1995.